ELSEVIER

Polymer 42 (2001) 5625–5632

polymer

www.elsevier.nl/locate/polymer

Resonance Raman spectroscopic investigation of the mechanism and kinetics of the degradation of *N*,*N*-hexamethylene bishexamide, a Nylon 6,6 model compound

H. Matsui[a,1], C.A. Schehr[a,2], J.J. Valentini[a,*], J.N. Weber[b]

[a]*Department of Chemistry, Columbia University, New York, NY 10027, USA*
[b]*DuPont Experimental Station, Wilmington, DE 19880, USA*

Received 12 October 2000; received in revised form 7 December 2000; accepted 7 December 2000

Abstract

We report a mechanistic study of the photo-oxidative degradation of *N*,*N*-hexamethylene bishexamide, a Nylon 6,6 model compound. Resonant Raman intensities of the amide and its previously identified enal degradation product are recorded as a function of the duration of the irradiation of the amide with 266 nm laser pulses. The time dependences of the Raman intensities are consistent with those predicted by a kinetic mechanism for photo-oxidation. In particular, the rate of formation of the enal, probed by monitoring the Raman intensity of its C=O stretch peak at 1680 cm^{-1}, agrees well with the rate of cleavage of the C–N bond in the amide, revealed by the time dependence of the intensity of the Am II (C–N stretch) vibration at 1537 cm^{-1}. Rate constants for important steps in the degradation mechanism are obtained from the analysis.

Keywords: Nylon; Degradation; Kinetics

1. Introduction

A major problem in studying polymer degradation is distinguishing the primary degradation products from those products that result from subsequent reactions [1]. It is sometimes a challenge even to secure conditions for which the type of degradation — hydrolytic, thermal, photolytic, or oxidative — can be established with certainty. For example, photo-absorption, leading to production of an excited electronic state of the polymer, can be followed by efficient energy transfer and internal conversion [2], dissipating the excitation energy as heat in the sample, and engendering a thermal, rather than photolytic, process. We recently reported UV resonance Raman experiments in which conditions could be maintained that allow the differentiation of photolytic degradation from thermal degradation, and we then used this approach to study thermal-oxidative, photolytic, and photo-oxidative degradation in amide polymers [3].

For Nylon 6,6 and *N*,*N*-hexamethylene bishexamide, a Nylon 6,6 model compound, we determined that upon irradiation with laser pulses of 266 nm UV light in an atmosphere containing molecular oxygen, photo-oxidative degradation took place. We used the spectral band positions and the excitation-wavelength-dependence of the band intensities of the degradation product in the UV resonance Raman spectra to identify it as an enal, a likely product of photo-oxidation. We observed that the product is not formed if the polymer is irradiated in an N_2 atmosphere, so a photolytic mechanism is not operative. A consideration of the energy deposition in the sample by the pulsed laser showed that the temperature rise that could be produced by laser heating, a few degrees, is too small to be significant, making a thermal-oxidative mechanism unlikely. And, the dependence of product formation on laser fluence was inconsistent with a thermally activated process. Further, no observable product was formed upon direct thermal heating of the samples in oxygen atmospheres, except when the model compound was heated above its melting point for several minutes. These observations rule out a thermal route for the laser-irradiated conditions. Thus, we determined that the degradation process we observed is purely a photo-oxidative one.

In this paper we report a mechanistic and kinetic study of this photo-oxidative degradation for this *N*,*N*-hexamethylene

* Corresponding author. Tel.: +1-212-854-7590; fax: +1-212-932-1289.
E-mail address: jjvl@chem.columbia.edu (J.J. Valentini).
[1] Present address. Department of Chemistry, University of Central Florida, Orlando, FL 32816, USA.
[2] Present address. Department of Chemistry, University of Chicago, Chicago, IL 60637, USA.

0032-3861/01/$ - see front matter
PII: S0032-3861(01)00004-0

bishexamide Nylon 6,6 model compound, for which we have identified the product and found it to be the same as that for the photo-oxidative degradation of Nylon 6,6 itself. Resonant Raman intensities of the vibrational bands of this bishexamide and its enal degradation product are recorded as a function of the duration of irradiation of the amide with the 266 nm laser pulses. The time dependence of the Raman intensities of the various vibrational bands are compared with what would be expected based on a reasonable mechanism for photo-oxidation. From analysis of the data, rate constants for various steps in the mechanism are obtained.

In the past, the kinetics of the UV photo-degradation of Nylon have been investigated by FTIR spectroscopy [4] or a combination of UV absorption, viscosity, and end-group analysis [5,6]. These experiments are obviously similar in intent to those we report here, but they are different in important ways. In the previous experiments, a high intensity continuous UV source, such as a mercury vapor or xenon arc lamp, was used for sample illumination, with exposure times of 10–10,000 h. Here we use Raman spectroscopy to follow reactant decay and product appearance, the latter facilitated by the substantial electronic resonance enhancement of the Raman scattering from the enal product. This detection methodology allows us to work in the regime of short-time, low-total-dosage UV exposure — fewer than 1000 laser pulses of 5 mJ energy each. In part this is because of the sensitivity afforded by the resonance enhancement of the product Raman scattering. It is also a consequence of the fact that the light used for probing the sample is the same as that used to degrade it.

2. Experimental

Resonant Raman spectra were taken using the Raman apparatus as described in our previous publications [3,7–9]. The fourth harmonic of an Nd:YAG laser (Continuum NY81C) operating with ≈6-ns-duration pulses at 10 Hz was the light source for the experiments. The 266 nm laser beam was loosely focused on the sample to a spot size of ≈5 mm diameter, and the Raman scattered light was collected at right angles to the incident beam direction. A one-meter monochrometer (Spex 14018) dispersed the Raman-scattered light, which was detected by a UV-enhanced CCD detector (Spex, Spectrum-1), and processed by Spex data acquisition hardware and software.

The *N*,*N*-hexamethylene bishexamide, as well as *N*-hexanoyl propionimide (vide infra), was made at the DuPont Company. The model amide compound was prepared by direct amidation of the corresponding acid and amine in an autoclave. The crude product was purfied by recrystallization and analyzed to be >99.5% pure by GC. The model imide was prepared by the reaction of hexanoyl chloride with propionamide at ≈273 K. The product was recrystallized and shown to be >98% pure by NMR. Other chemicals (vide infra), such as *trans*-2-heptenal and isobutylamide, were obtained from Aldrich and used without further purification.

For the kinetics studies, samples of *N*,*N*-hexamethylene bishexamide were prepared by pouring a methanol slurry of the compound onto an aluminum disk. Evaporation of the methanol produced a uniform, flat, mechanically stable sample. The sample was mounted on a computer-controlled rotation/translation stage that made it possible to select a specific, known area of the sample for degradation/optical probing, and to bring a fresh area into the irradiation region at will. These samples were studied while open to the ambient atmosphere. Reference spectra of various samples were obtained with free-standing powders in a closed quartz microcell under an atmosphere of ambient air.

Identification of the product of the degradation was done as reported by us before [3], irradiating the sample with 1200 shots of the laser with the 266 nm pulse energy set at 15 mJ. The resonance Raman spectra of the polymer was recorded both before and after the degradation-inducing irradiation, with an exposure (600 pulses) half as long as that for the degradation, at a pulse energy (1.5 mJ) one-tenth as large.

For analysis of the time dependence of the Raman spectra, photo-degradation and Raman spectral probing were done simultaneously. Raman scattered light was collected on every laser pulse that was incident on the sample, and thus there was no separation of the photo-degradation and probing. The Raman signal was integrated for exposure times of 0–1000 laser shots at 5 mJ per pulse.

3. Experimental results

3.1. Product identification

Identification of the product of the degradation of Nylon 6,6 and the *N*,*N*-hexamethylene bishexamide Nylon 6,6 model compound was the subject of our previous report [3]. Here we review that work to give the background necessary for understanding the mechanistic and kinetic study we describe in this publication. Raman spectra of *N*,*N*-hexamethylene bishexamide, excited at 266 nm before and after 266 nm degradation irradiation, are presented in Fig. 1, which covers the region between 1150 and 1750 cm^{-1}, and Fig. 2, which shows the region between 2600 and 3400 cm^{-1}. There are no bands in the spectral region between 1750 and 2600 cm^{-1}.

Although the same wavelength is used for both photo-degradation and resonant Raman excitation, the total laser pulse energy used to record the Raman spectra before the photo-degradation irradiation and after it is not sufficient to produce measurable amounts of the product. Thus, the low pulse energy, short irradiation time 266 nm Raman excitation adequately characterizes the samples "before" and "after" degradation without ambiguity. After degradation, a peak at approximately 1680 cm^{-1} that is due to a degradation product appears clearly in the Raman spectrum. We

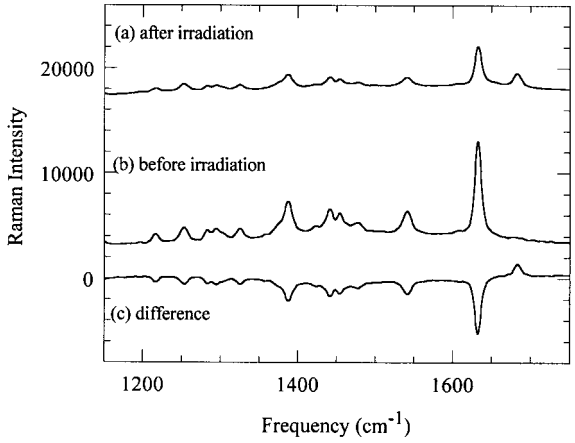

Fig. 1. Raman spectra (266 nm excitation) of *N,N*-hexamethylene bishexamide between 1150 and 1750 cm^{-1}: (a) after UV-irradiation at 266 nm, with 15 mJ per pulse at 10 pulses per s for 2 min; (b) without UV-irradiation; and (c) spectrum (a) minus spectrum (b).

have shown previously that this band can be assigned to the C=O stretch of an enal product [3]. Except for that band, the before spectrum (b) and the after spectrum (a) are both dominated by vibrational bands of the Nylon 6,6 model compound. These bands are the characteristic Am I (C=O stretch) and Am II (primarily C–N stretch) peaks, as well as the CH_3 and CH_2 deformations that occur at 1640, 1537, 1434, and 1379 cm^{-1}. Vibrational modes at 2857, 2883, 2912, and 2947 cm^{-1} are assigned as CH stretch, and that at 3300 cm^{-1} is the NH stretch from the Nylon 6,6 model compound [10].

Comparison of the after spectra (a) and before spectra (b) in Figs. 1 and 2 shows that the degradation reduces the intensity of the spectral peaks associated with the Nylon 6,6 model compound. This is revealed clearly by subtracting the before irradiation spectrum from the after irradiation spectrum, to give the difference spectrum (c). The loss of the model compound caused by the irradiation is shown by the negative-going peaks in the difference spectrum.

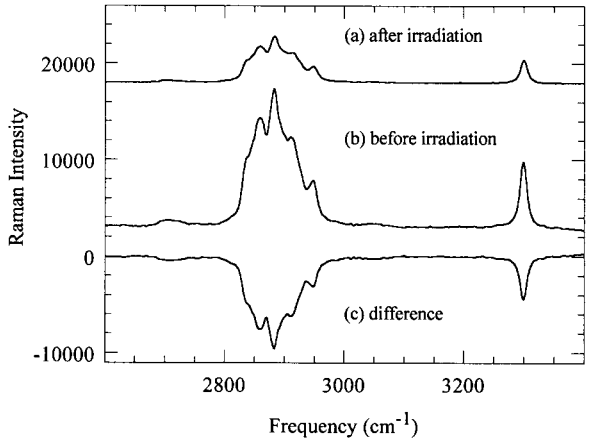

Fig. 2. Same as in Fig. 1, but for the spectral region from 2600 to 3400 cm^{-1}.

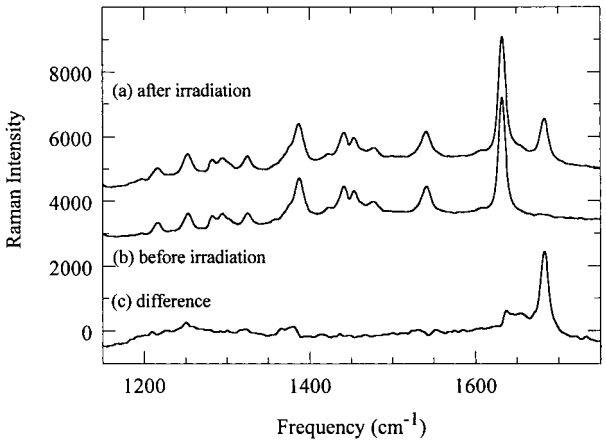

Fig. 3. Same as in Fig. 1, but with the spectrum obtained after UV-irradiation scaled so that the spectral intensities of the CH_2 twist, rock, and deformation bands located around 1400 cm^{-1} match the intensities of those same bands in the spectrum without irradiation.

As described by us previously, the enal product also shows a peak at 1640 cm^{-1}, but this peak is not evident in the difference spectrum of Fig. 1. This product peak is masked by the loss in intensity at 1640 cm^{-1} associated with the decrease in the Am I band of the Nylon 6,6 model compound during irradiation, a loss that gives a bigger change in the spectrum than does the gain due to the enal product appearance. However, the contribution of the enal product to the spectral intensity at 1640 cm^{-1} becomes observable when the after spectrum is scaled to compensate for loss of intensity in the amide modes prior to subtracting the before spectrum from the after spectrum. This scaling produces a before–after difference that would be a null except for the contribution of product spectral intensity. We do the necessary scaling using the intensities of the CH_2 twist, rock, and deformation modes, and the results are shown in Fig. 3. This normalized difference spectrum shows the appearance of only the two enal peaks; there are no other spectral peaks between 500 and 3500 cm^{-1}.

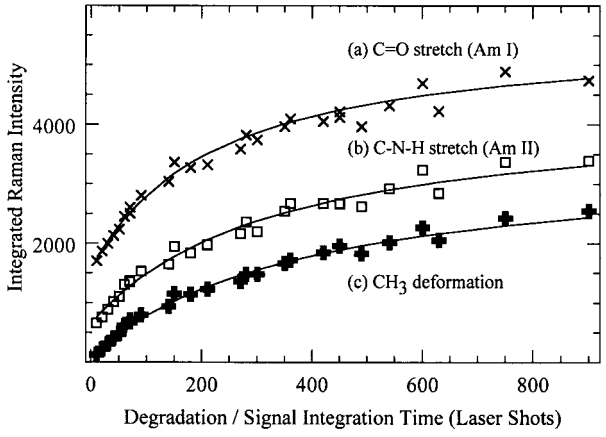

Fig. 4. Plots of the integrated Raman intensities of the Am I, Am II, and CH_3 deformation modes of the *N,N*-hexamethylene bishexamide as a function of degradation time. The symbols are the experimental measurement. The solid curves are the fits of Eq. (14) to the experimental data.

3.2. Time dependence of degradation

Time-integrated Raman signal intensities for the 1680 cm^{-1} enal product peak and for six of the vibrational bands of the *N*,*N*-hexamethylene bishexamide parent are shown as a function of irradiation time, which is also the Raman spectrum acquisition time, in Figs. 4–6. It is important to remember that the time-integrated Raman signal intensity, the intensity at a particular number of laser shots, *N*, on any one of these plots, is not proportional to the molecular concentration at a particular time. Rather, the integrated signal is, as its name implies, proportional to the molecular concentration integrated over the course of the total of the *N* laser shots. That is:

$$\text{Integrated Raman Signal } (N) = \sum_{n=1}^{N} a(\text{species})[\text{species}(n)]$$

$$= a(\text{species}) \sum_{n=1}^{N} [\text{species}(n)] \cong a(\text{species}) \times \int_{t=0}^{t=t_N} [\text{species}(t)]\, dt \qquad (1)$$

Here, a(species) is a proportionality constant relating the concentration of a particular species to the Raman signal from it. This constant is determined empirically. The quantities [species(n)], [species(t)] are, respectively, the concentrations of that species at laser shot n or time t. Eq. (1) shows why the integrated Raman signal can increase with increasing time (increasing number of laser shots), even for a species whose concentration is decreasing with time.

4. Mechanistic analysis

A possible scheme for the photo-oxidative degradation is [3]:

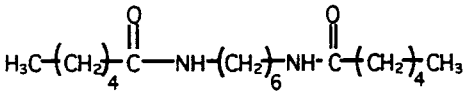

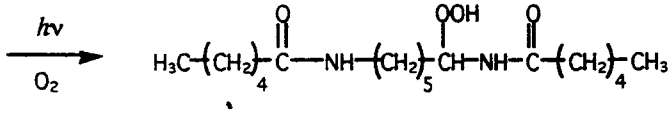

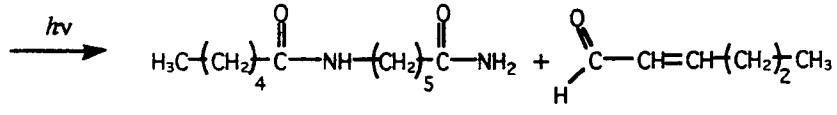

A mechanism for such a scheme is:

Initiation:

$$\text{Initiator} + h\nu \xrightarrow{k_0} \text{Init}\cdot + \text{X}\cdot \qquad \text{(a)}$$

$$\text{Init}\cdot + \text{AmH} \xrightarrow{k_1} \text{Am}\cdot + \text{Init}\cdot\text{–H} \qquad \text{(b)}$$

Propagation:

$$\text{Am}\cdot + O_2 \xrightarrow{k_2} \text{AmOO}\cdot \qquad \text{(c)}$$

$$\text{AmOO}\cdot + \text{AmH} \xrightarrow{k_3} \text{AmOOH} + \text{Am}\cdot \qquad \text{(d)}$$

Subsequent reactions:

$$\text{AmOOH} + h\nu \xrightarrow{k_4} \text{enal} + \text{primary amide} + H_2O \qquad \text{(e)}$$

$$\text{AmOOH} + h\nu \xrightarrow{k_4'} \text{AmO}\cdot + \cdot\text{OH} \qquad \text{(f)}$$

$$\text{enal} \xrightarrow{k_5} \text{secondary product} \qquad \text{(g)}$$

Termination:

$$\text{Am}\cdot + \text{Am}\cdot \xrightarrow{k_6} \text{Am}_2 \qquad \text{(h)}$$

$$\text{AmOO}\cdot + \text{AmOO}\cdot \xrightarrow{k_7} \text{AmOOAm} + O_2 \qquad \text{(i)}$$

In this mechanism the photolysis of the AmOOH in step (e) yields the enal product. It can also yield (through step (f)) an ·OH radical that is one particular Init· species in step (b). This makes the mechanism nominally autocatalytic photolytically. However, it appears that the concentration of the AmOOH does not reach levels high

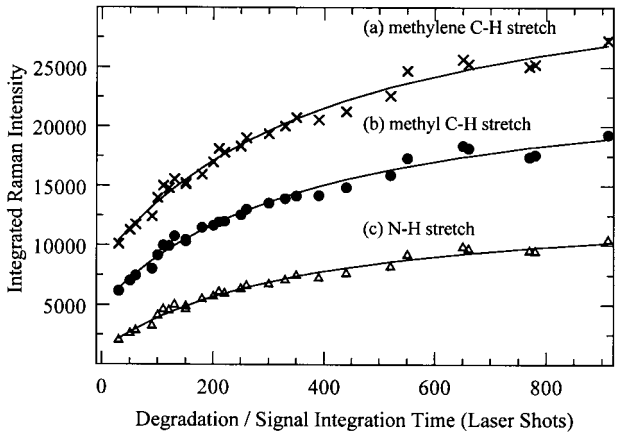

Fig. 5. Same as Fig. 4, except for two C–H stretch bands and the N–H stretch band of the *N*,*N*-hexamethylene bishexamide.

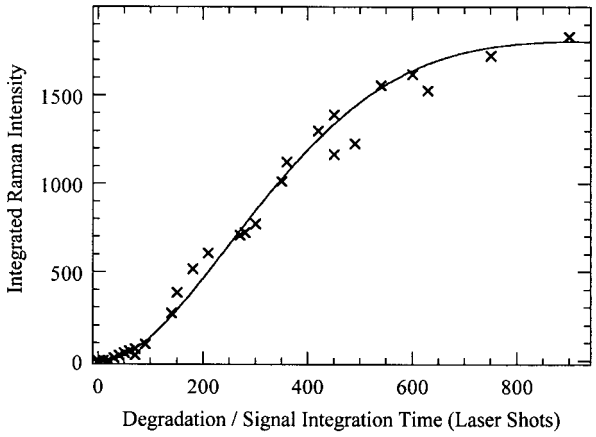

Fig. 6. Same as Fig. 4, except for the C=O stretch band of the enal product of the degradation, and using Eq. (15) for the fit to the short-time (200 shots or less) data and Eq. (16) for the fit to the longer time (more than 200 shots) data.

enough for this autocatalysis to have any quantitative effect on the kinetics of the degradation. First, the kinetics of the polyamide decay and the enal appearance are adequately fit (vide infra) by the mechanism neglecting the autocatalysis. If the AmOOH photolysis to yield ·OH was important, the mechanism would not fit the observations at both short times, when the AmOOH has not built up, and at long times, when it has. Second, the AmOOH peroxide was not observed in any of our Raman spectra. Such a species should give a strong Raman band around 900 cm^{-1}, associated with the peroxide O–O stretch [10]. Its absence from our spectra for all irradiation times indicates that its concentration is both low and effectively constant. This validates making a steady-state approximation for it, as well as for the even more reactive intermediates Am· and AmOO·. Doing so we have:

$$\frac{d[Am\cdot]}{dt} = k_1[AmH] - k_2[Am\cdot][O_2] + k_3[AmOO\cdot][AmH] - k_6[Am\cdot]^2 = 0 \quad (2)$$

$$\frac{d[AmOO\cdot]}{dt} = k_2[Am\cdot][O_2] - k_3[AmOO\cdot][AmH] - k_7[AmOO\cdot]^2 = 0 \quad (3)$$

$$\frac{d[AmOOH]}{dt} = k_3[AmOO\cdot][AmH] - k_4[AmOOH] = 0 \quad (4)$$

Eqs. (2) and (3) yield:

$$k_1[AmH] - k_6[Am\cdot]^2 - k_7[AmOO\cdot]^2 = 0 \quad (5)$$

Now, the recombination rate coefficients k_6 and k_7 should be comparable in magnitude, but [AmOO·] and [Am·] are not. Rather, [AmOO·] will be much larger than [Am·], since the rate of reaction (c) will greatly exceed that of reaction (d). The latter will be limited by solid-state diffusion, the former only by the gaseous diffusion of molecular oxygen, which is in large excess under the conditions of these experiments. Thus, the second term in Eq. (5) can be neglected in comparison with the third, giving:

$$[AmOO\cdot] = \left(\frac{k_1}{k_7}\right)^{1/2}[AmH]^{1/2} \quad (6)$$

The rate of degradation for the *N*,*N*-hexamethylene bishexamide is:

$$\frac{d[AmH]}{dt} = -k_1[AmH] - k_3[AmOO\cdot][AmH] \quad (7)$$

Substituting Eq. (6) into Eq. (7) and integrating yields:

$$[AmH] = \left(\frac{-k_3}{(k_1k_7)^{1/2}} + C\,e^{-k_1t/2}\right)^{-2} \quad (8)$$

where C is a constant and t is degradation time.

The kinetic equation for the enal is:

$$\frac{d[enal]}{dt} = k_4[AmOOH] - k_5[enal] \quad (9)$$

Combing Eqs. (4) and (6) gives:

$$k_4[AmOOH] = k_3\left(\frac{k_1}{k_7}\right)^{1/2}[AmH]^{3/2} \quad (10)$$

Using Eq. (10) to eliminate [AmOOH] from Eq. (9) yields d[enal]/dt, as a function of [AmH] and [enal]:

$$\frac{d[enal]}{dt} = k_3\left(\frac{k_1}{k_7}\right)^{1/2}[AmH]^{3/2} - k_5[enal] \quad (11)$$

This equation cannot be solved directly, but its long-time and short-time behavior can be separated. (The results of the analysis that follows demonstrate the validity of this separation.) For times short enough for the enal concentration to be sufficiently small to make k_5[enal] negligible, we have only the production term, $k_3(k_1/k_7)^{1/2}[AmH]^{3/2}$, in Eq. (11). For times long enough for the production of the enal to be balanced by its destruction, d[enal]/dt will be near zero,

Table 1
Kinetic rate constants for the photo-oxidative degradation mechanism, derived from observations of the time dependence of the Raman intensity of selected vibrational bands of *N,N*-hexylmethylxene bishexamide and the enal product

Vibrational modes for Nylon 6,6 model	Vibrational frequencies (cm^{-1})	$10^4 \times k_1$ (s^{-1})	$k_3/(k_1k_7)^{1/2}$ ($M^{-1/2}$)	C
CH_3 symmetric deformation	1379	2.28(3)	1.04(1)	1.08(1)
CH_3, CH_2 deformation	1434	2.17(8)	1.08(3)	1.13(3)
C–N stretch (Am II)	1537	2.28(8)	1.09(3)	1.12(3)
C=O stretch (Am I)	1640	2.19(3)	1.09(2)	1.11(2)
C=O stretch for product	1680	2.35(3)	1.00(1)	1.01(1)
Symmetric C–H stretch ($-CH_2-$)	2857	2.17(3)	1.06(1)	1.10(1)
Symmetric C–H stretch ($-CH_3$)	2883	2.17(2)	1.06(1)	1.11(1)
Antisymmetric C–H stretch ($-CH_2-$)	2912	2.22(9)	1.07(4)	1.11(4)
Antisymmetric C–H stretch ($-CH_3$)	2947	2.20(9)	1.07(4)	1.11(4)
N–H stretch	3300	2.20(5)	1.07(1)	1.11(1)

and a steady-state approximation for it can be made. In the short-time domain we thus have:

$$[\text{enal}] = \int_0^t k_3\left(\frac{k_1}{k_7}\right)^{1/2}[\text{AmH}]^{3/2}\,dt'$$
$$= (-k_{\text{eff}} + C\,e^{-k_1t/2})^{-2} - \frac{2}{k_{\text{eff}}}(-k_{\text{eff}} + C\,e^{-k_1t/2})^{-1}$$
$$- \frac{2}{k_{\text{eff}}^2}\ln(-k_{\text{eff}} + C\,e^{-k_1t/2}) + \frac{k_1}{k_{\text{eff}}^2}t \qquad (12)$$

where $k_{\text{eff}} = k_3/(k_1k_7)^{1/2}$, while in the long-time domain:

$$[\text{enal}] = \frac{k_3}{k_5}\left(\frac{k_1}{k_7}\right)^{1/2}[\text{AmH}]^{3/2} \qquad (13)$$

To compare the expectations of the model with the actual observations, and to extract values of the rate constants in the model from the data, we need to integrate Eqs. (8), (12), and (13), since the integrated Raman intensity data we record are (Eq. (1), vide supra) proportional to the species concentration integrated from time zero to time t. Those integrals are:

$$\int_0^t [\text{AmH}]dt' = \frac{2}{k_1k_{\text{eff}}}(-k_{\text{eff}} + C\,e^{-k_1t/2})^{-1}$$
$$- \frac{2}{k_1k_{\text{eff}}^2}\ln(-k_{\text{eff}} + C\,e^{-k_1t/2}) + \frac{t}{k_{\text{eff}}^2} \qquad (14)$$

$$\int_0^t [\text{enal}]_{\text{short time}}\,dt' = \int_0^t\int_0^{t'} k_3\left(\frac{k_1}{k_7}\right)^{1/2}[\text{AmH}]^{3/2}\,dt'dt''$$
$$= \frac{2}{k_1k_{\text{eff}}}(-k_{\text{eff}} + C\,e^{-k_1t/2})^{-1}$$
$$- \frac{6}{k_1k_{\text{eff}}^2}\ln(-k_{\text{eff}} + C\,e^{-k_1t/2}) + \frac{k_1}{2k_{\text{eff}}^2}t^2 - \frac{3}{k_{\text{eff}}^2}t \qquad (15)$$

$$\int_0^t [\text{enal}]_{\text{long time}}\,dt' = \int_0^t \frac{k_3}{k_5}\left(\frac{k_1}{k_7}\right)^{1/2}[\text{AmH}]^{3/2}\,dt'$$
$$= \frac{1}{k_5}(-k_{\text{eff}} + C\,e^{-k_1t/2})^{-2}$$
$$- \frac{2}{k_5k_{\text{eff}}}(-k_{\text{eff}} + C\,e^{-k_1t/2})^{-1}$$
$$- \frac{2}{k_5k_{\text{eff}}^2}\ln(-k_{\text{eff}} + C\,e^{-k_1t/2}) + \frac{k_1}{k_5k_{\text{eff}}^2}t \qquad (16)$$

For fitting to the Raman data we set the "short time" to be that at less than 200 laser shots, while the "long time" was greater than 200 laser shots.

The results of fitting these equations to the experimental integrated Raman signals are shown as solid curves in Figs. 4–6. Kinetic rate coefficients from the fit to each vibrational band are summarized in Table 1. The consistency of the k_1, $k_3/(k_1k_7)^{1/2}$, and C parameters for all vibrational bands supports the correctness of this proposed mechanism. The model mechanism provides a good description of the temporal dependence of the Raman intensities (proportional to species concentration) for all the vibrational bands that we characterized. More importantly, the data are all well fit by a single consistent set of rate coefficients. This is illustrated by Fig. 7, in which we compare the measured integrated Raman intensity of the Am II band of the *N,N*-hexamethylene bishexamide with the intensity predicted using the kinetic parameters k_1, $k_3/(k_1k_7)^{1/2}$, and C that come from fitting the enal integrated Raman intensity. The agreement is good, and in fact the enal parameters do almost as good a job of describing the amide decomposition as do the parameters that are fit to the amide data directly.

That there is a single set of kinetic parameters that fits both the increase in enal concentration with time and the decrease of amide with time is also important for another reason. It shows that the proportionality constant a in Eq. (1) is time-independent. This means that the degradation does not change the optical properties of the sample in a way that alters the relation between the concentrations and Raman band intensities.

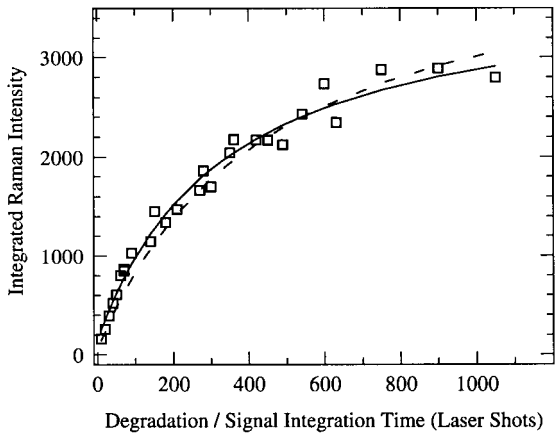

Fig. 7. Comparison of two fits to the experimental integrated Raman intensity as a function of time (open squares) for the Am II band of the *N*,*N*-hexamethylene bishexamide. The solid curve is the best-fit to this experimental data, and is identical to the solid curve fit to this data in Fig. 4. The dashed curve is the time dependence predicted for the Am II band based on the kinetic parameters (Table 1) that provide the best-fit to the time dependence of the enal product appearance.

Using the tabulated values of k_1, $k_3/(k_1k_7)^{1/2}$, and C in Eqs. (8) and (12) gives us the time variation of the concentration of the amide and the enal product, which is shown as the time variation of the Raman intensity of various bands in Figs. 8–10. There are two curves shown in Fig. 10, one labeled "Empirical" and the other "Kinetic Model". The latter is the result of calculating the enal concentration via Eq. (12). The former is obtained by fitting a polynomial to the enal integrated Raman intensity and then differentiating. The difference between these two is representative of the uncertainty (or error) introduced by the fact that we had to describe the enal time dependence in terms of separate short-time and long-time domains. The data in these three figures is presented here because it shows what the time dependence of the Raman signals, and thus the species concentrations, would be if they were measured. We hasten

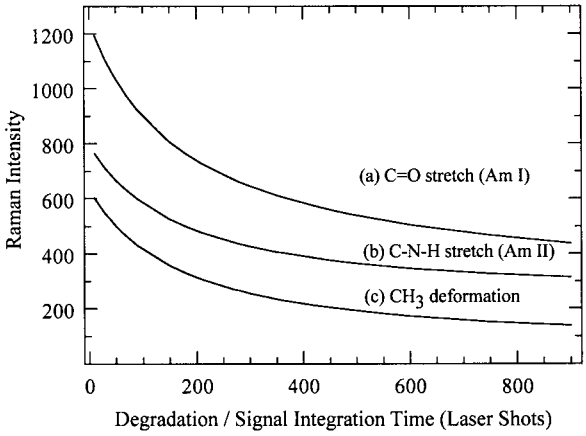

Fig. 8. The time-dependent Raman intensities (proportional to *N*,*N*-hexamethylene bishexamide concentration) for the C=O, C–N, and CH_3 deformation modes of the *N*,*N*-hexamethylene bishexamide.

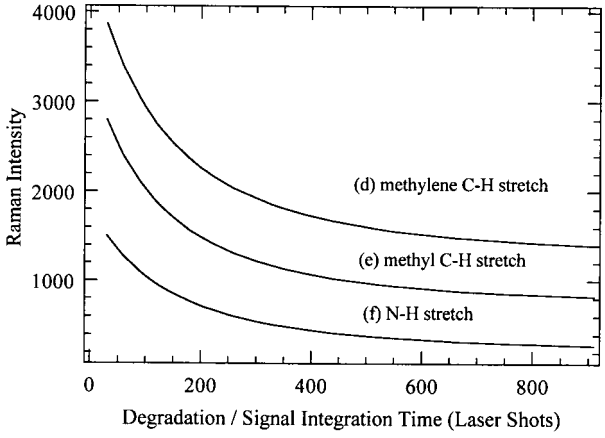

Fig. 9. Same as in Fig. 8, except for the $-CH_3$ group symmetric stretch, $-CH_2-$ group symmetric stretch, and N–H stretch bands of the *N*,*N*-hexamethylene bishexamide.

to add that these quantities are not directly measured here, nor do they have to be in order to establish the mechanism. The integrated intensities are sufficient for this purpose.

The most prominent feature of the kinetic rate constants (Table 1) that we obtain is that they are the same irrespective of the identity of the band we select. This observation bears some discussion. In the photo-oxidation process, only some of the bonds of the *N*,*N*-hexamethylene bishexamide are transformed; many are left untouched. In fact, of the two amide groups in the bishexamide only one need be oxidized to yield the enal. And the product formed with the enal is itself an amide. Why should all the bands show the same temporal behavior?

The answer to this question has two parts. First, even though photo-oxidation only affects some of the bonds, it does destroy the *N*,*N*-hexamethylene bishexamide, and thus eliminates the Raman intensity from any and all its vibrational bands. Second, although both the products contain

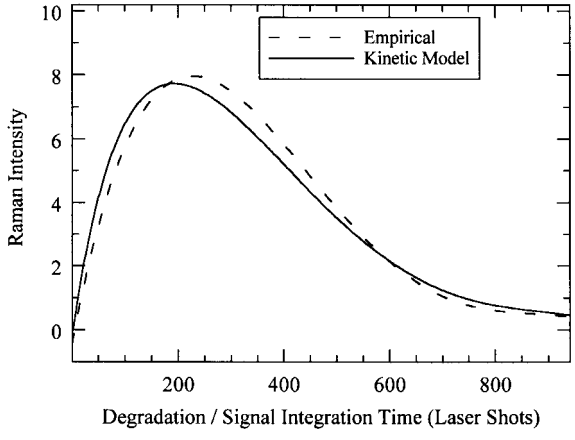

Fig. 10. Time-dependent Raman intensity of the C=O stretch of the enal product (proportional to enal concentration). The solid curve is the time dependence in the kinetic model (see text); the dashed curve is the result of differentiation of a polynomial fit to the experimental data shown in Fig. 6.

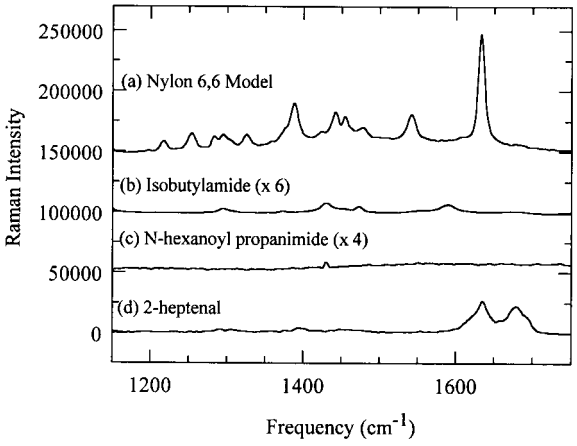

Fig. 11. Raman spectra (266 nm excitation) of *N,N*-hexamethylene bishexamide, isobutylamide, *N*-hexanoyl propionimide, and 2-heptenal between 1150 and 1750 cm^{-1}.

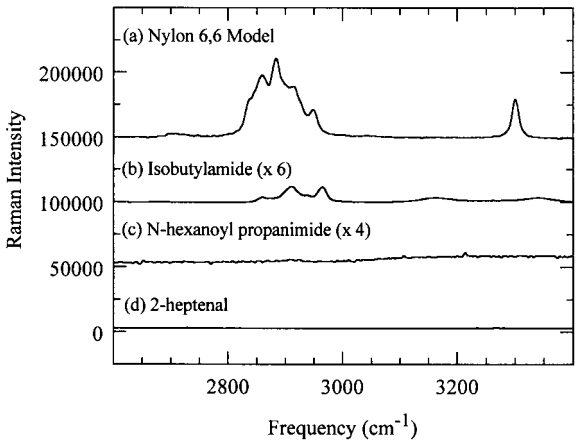

Fig. 12. Same as Fig. 11, but for the region between 2600 and 3400 cm^{-1}.

some of the same functional groups as the amide reactant, it is unlikely that either product would give a Raman spectrum that interferes with the spectrum of the amide reactant.

To demonstrate this, we compare the 266 nm resonance Raman spectra of the *N,N*-hexamethylene bishexamide, isobutylamide, *N*-hexanoyl propionimide ($H_{12}C_5CONH$-COC_3H_5), and *trans*-2-heptenal ($H_3C(CH_2)_3CH{=}CHCHO$). The isobutylamide provides a model of the behavior of the primary amide group in the diamide product, the propionimide models the behavior of the secondary amide in the product, and the heptenal is a prototype of the enal product. Figs. 11 and 12 show the Raman spectra of all four compounds.

These figures show that, with one exception, the 266 nm Raman spectra of the three compounds that serve as prototypes of the products do not interfere with the Raman spectrum of the *N,N*-hexamethylene bishexamide. The amide-containing molecules have too low intensity or have bands that are shifted relative to those for the Nylon 6,6 model. This observation is consistent with expectations [11,12]. Heptenal has too little intensity except in a band at 1640 cm^{-1}, which overlaps the Am I (C=O) of the reactant. However, under the conditions of our measurements the extent of degradation (vide supra) is sufficiently small for the intensity of this band to be too low to make it a significant interference with the reactant band intensity.

We note in passing that a comparison of the spectra in Figs. 3 and 11, shows different relative intensities for the 1680 and 1640 cm^{-1} peaks in the heptenal and degradation product spectra. The spectrum of Fig. 11 is for neat heptenal, but the heptenal degradation product is in an amide enviroment of the model compound. The spectrum of heptenal in dimethlyacetamide, which mimics the environment of heptenal in Nylon 6,6 and the model compound, shows that the 1640 and 1680 cm^{-1} band intensities are different from those in neat heptenal and are concentration-dependent [3].

5. Conclusions

Observations of the time-dependent changes of Raman intensities of selected vibrational bands of a Nylon 6,6 model compound and its enal product are found to be consistent with a mechanism for photo-oxidation. Quantitative analysis of these band intensities yields values for the rate constants of some of the steps in the mechanism.

Acknowledgements

This research is supported by the DuPont Company. The authors thank Nancy Singletary and Scott Hutchinson for preparation of the model amide used for this study.

References

[1] Kohan MI. Nylon plastics handbook. New York: Hanser/Gardner, 1995 (p. 49).
[2] Rabek JF. Photodegradation of polymers. New York: Springer, 1996 (p. 10).
[3] Matsui H, Arrivo SM, Valentini JJ, Weber JN. Macromolecules 2000;33:5655–64.
[4] Do CH, Pearce EM, Bulkin BJ, Reimschuessel HK. J Polym Sci, Polym Chem Ed 1987;25:2301–21.
[5] Moore RF. Polymer 1963;4:493–513.
[6] Karstens T, Rossbach V. Makromol Chem 1989;190:3033–53.
[7] Triggs NE, Valentini JJ. J Phys Chem 1992;96:6922–31.
[8] Triggs NE, Bonn RT, Valentini JJ. J Phys Chem 1993;97:5535–40.
[9] Triggs NE, Valentini JJ. Isr J Chem 1994;34:89–93.
[10] Lin-Vien D, Colthup NB, Fateley WG, Grasselli JG. The handbook of infrared and Raman characteristic frequencies of organic molecules. New York: Academic Press, 1991.
[11] Arrivo SM, Valentini JJ, Weber JN. Unpublished result.
[12] Hendra PJ, Agbenyega JK. The Raman spectra of polymers. New York: Wiley, 1993 (p. 50–1).